Simbol-X Telescope: Passive Shielding Systems Scientific Trade-Off Studies

V 4.0

INAF / IASF Internal Report n. 448/2006

G. Malaguti(1), V. Fioretti(1,2), S. Mereghetti(3), G. Pareschi(4)

(1)INAF/ IASF-Bologna
(2)Dipartimento di Astronomia, Università di Bologna
(3)INAF/ IASF-Milano
(4)INAF/ Osservatorio Astronomico di Brera

Change history

Version	Date	Notes
1.0	Oct 12th, 2006	1st Issue
2.0	Oct 19th, 2006	Telescope (DSC and MSC) geometry generalized to 3-dimension, translating maximum aperture background component into requirements for the residual solid angle.
3.0	Nov 10th, 2006	Cosmic diffuse background non-uniformity on the detection plane calculated for different energies, for a circular collimator geometry in the case of a non complete shielding.
4.0	Dec 6th, 2006	Mirror optics module dimension increased to D_{opt}=80cm. Addition of a more precise solid angle evaluation for the edge of the field of view. Addition of absorbers mass evaluation.

1. Introduction and aim

The fundamental scientific objectives of the Simbol-X telescope (as defined in the *Simbol-X Top Level Scientific Requirements* Document) require a sensitivity of the order of <1μCrab (for deep, T_{int}~10^6s, survey observations) in the 10-40 keV band. This implies the necessity of great care in the minimization of the background radiation at high energy.

The background can be broadly divided into two main components: (a) the diffuse Cosmic X-ray Background (CXB) reaching the detector either from directions outside the focussing system or leaking through the shields, and (b) the prompt and delayed activation components due to the interaction of high energy photons or particles.
The study of component (b) requires detailed modelling and prototypal analysis in order to finely tune the choice of geometry, composition, and logical philosophy of the active shields. On the contrary, the critical parameter for the minimization of component (a) can be identified with the detector opening solid angle, Ω_{CXB}, defined by the shielding system. This is clearly explained in Figure 1 which shows some of the recent measurements of the background spectra in the Simbol-X energy range, normalized to an opening angle Ω_{CXB} between 3×10^{-5} and 1×10^{-3} sr, with the addition of an energy independent value to mimic the contribution of the hadronic component.

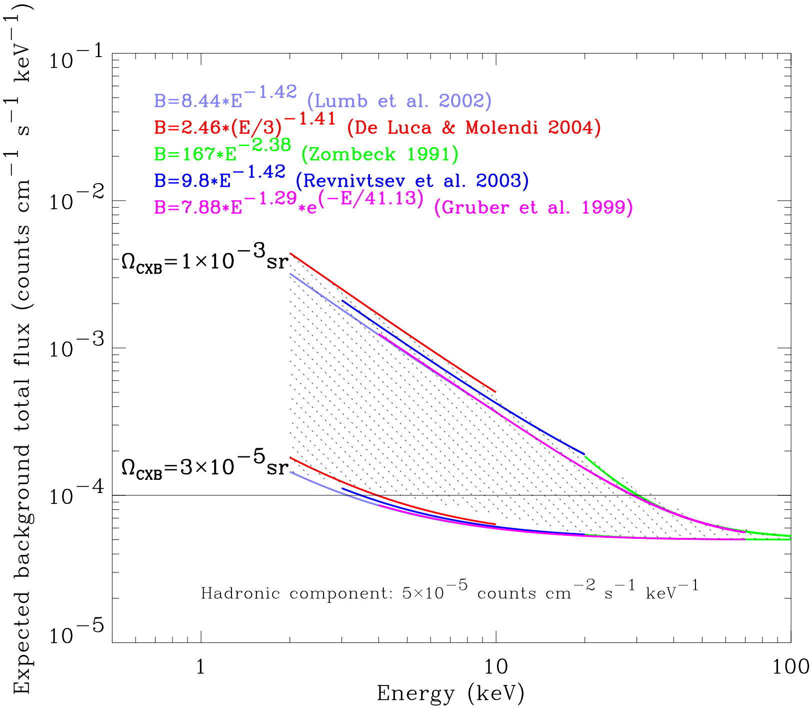

Figure 1:

Expected background count spectrum calculated normalizing the available CXB measurements (expressed in units of counts cm^{-2} s^{-1} keV^{-1} sr^{-1}) to a detector opening solid angle Ω_{CXB}, between 3×10^{-5} and 1×10^{-3} sr, plus the addition of an energy independent hadronic component equal to $5\cdot10^{-5}$ counts cm^{-2} s^{-1} keV^{-1}. The superimposed line at $1\cdot10^{-4}$ counts cm^{-2} s^{-1} keV^{-1} indicates the upper limit on the total background required to reach a sensitivity ~0.5μCrab in the 10-40 keV band as requested by the Simbol-X scientific objectives for the deep survey observations (T=1Ms).

Figure 1 shows that the required limit on the total Simbol-X background to be less than 10^{-4} counts cm^{-2} s^{-1} keV^{-1} at ~30 keV, implies an opening angle Ω_{CXB}<10^{-3} sr. On the other hand, the same background limit applied over the entire Simbol-X energy range translates into a Ω_{CXB} that has to be >30 times smaller.
Moreover, if on one side the formation flying scenario hampers the shielding the whole telescope by means of the canonical "tube", on the other it does open the possibility of implementing novel design solutions. In particular, see Malaguti et al. (2005) for details, it allows to share the shielding between the Detector SpaceCraft (DSC) and the Mirror SpaceCraft (MSC).

This Technical Note is a first attempt aimed at a detailed quantitative exploration of the phase space defined by the fundamental telescope design parameters associated with the MSC and DSC baffles geometry and composition.

In Section 2 we give the basic definitions and assumptions adopted for this note. In Section 3 the key points of the chosen analytical approach are described. In Section 4 and 5 we show the first results which can also be considered as fundamental inputs for the technical feasibility studies to be performed during Simbol-X Phase-A: Section 4 addresses the possible geometry trade-off for a "perfect shielding" scenario at all energies; Section 5 shows a trade-off analysis of non-perfect shielding geometries, with the evaluation of the residual aperture component background non-uniformity on the detection plane in different energy bands.

2. Definitions and basic assumptions

Figure 2 shows the basic simplified geometry of the Simbol-X telescope assembly. The main quantities defined in Figure 2 and then used for the trade-off analysis are the following:

D_{opt}: External mirror shell diameter.
R_{skirt}: Skirt (MSC baffle) dimension, all around D_{opt}.
D_{MSC}: $D_{opt} + 2 \cdot R_{skirt}$
R_{MSC}: $D_{MSC}/2$
H: Collimator (DSC baffle) height.
D_{det}: Focal plane detector dimension.
s: Focal plane / collimator separation.
$\Delta\theta$: Detector opening angle, corresponding to Ω_{CXB} sr.
FL: Telescope focal length.

On the basis of the current feasibility scenarios, we have done the following assumptions:

D_{opt}: 80cm
R_{skirt}: Variable (technical feasibility to be assessed).
H: Variable (technical feasibility to be assessed).
D_{det}: 8cm.
s: Large enough to avoid vignetting by the collimator walls (see below).
FL: 20m.

In this first study we have considered the MSC baffle (skirt) being perpendicular to the telescope axis, and the collimator walls parallel to it. This latter assumption is one of the reasons why we have chosen, at least at the present still preliminary stage, to work under the conservative hypothesis of considering the whole detection plane also for small Ω_{CXB} values (see the trigonometric formulas used in Section 3). This conservative approach also allows to compensate the possible mis-alignment between MSC and DSC during observations.

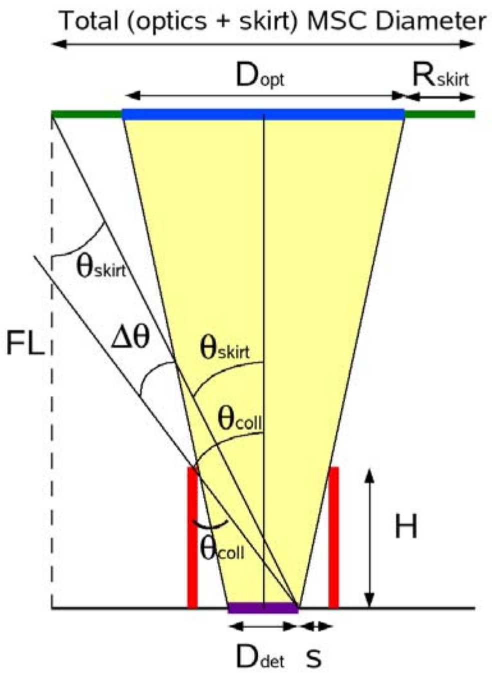

Figure 2:

The basic simplified geometry of the Simbol-X telescope assembly is shown. The **blue** horizontal line on the top indicates the external optics diameter, D_{opt}. The top external **green** lines represent the *skirt*, or MSC baffle, which adds a further R_{skirt} all around D_{opt}. The **purple** line on the bottom is the detection plane which has a dimension of D_{det} and is separated by *s* from the collimator (or DSC baffle) walls (**red** lines) of height *H*. *FL* is the telescope focal length.
For the derivation of all the angles indicated in the figure, see Section 3.

The separation *s* between DSC baffle and detector edge is necessary to avoid direct shadowing of the focussed photons. Adopting the notation defined in Figure 1, we have that:

$$s \geq \frac{H \cdot (D_{opt} - D_{det})}{2 \cdot FL}$$

3. Analytical approach

For a given detector opening angle Ω_{CXB}, the required total (D_{opt}+2·R_{skirt}) MSC diameter clearly depends on the DSC baffle height (H).
Following a simple trigonometric approach we have that:

$$\Delta\theta = \theta_{coll} - \theta_{skirt} = \mathrm{arctg}\left[\frac{D_{det}}{H} + \frac{D_{opt} - D_{det}}{2 \cdot FL}\right] - \mathrm{arctg}\left[\frac{D_{MSC} + D_{det}}{2 \cdot FL}\right],$$

and therefore:

$$D_{MSC} = 2 \cdot FL \cdot \mathrm{tg}\left[\mathrm{arctg}\left(\frac{D_{det}}{H} + \frac{D_{opt} - D_{det}}{2 \cdot FL}\right) - \Delta\theta\right] - D_{det},$$

and

$$R_{skirt} = \frac{D_{MSC} - D_{opt}}{2},$$

while Ω_{CXB} is given by:

$$\Omega_{CXB} = \int_0^{2\pi} \int_{\theta_{skirt}}^{\theta_{coll}} \mathrm{sen}\theta \, d\theta \, d\varphi = 2\pi \int_{\theta_{skirt}}^{\theta_{coll}} \mathrm{sen}\theta \, d\theta = 2\pi \cdot (\cos\theta_{skirt} - \cos\theta_{coll}) \cong 2\pi \cdot \Delta\theta \cdot \sin\theta_{coll}$$

The same shielding can be obtained by means of a different configuration, which is described in Figure 3. This configuration includes the presence of two co-planar and concentric discs placed above the detection plane, which allow for a significantly shorter collimator tube.

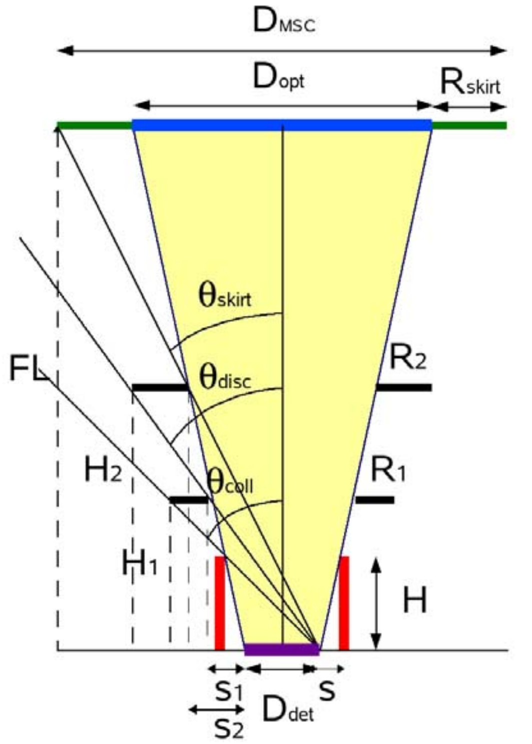

Figure 3:

The basic simplified geometry of the Simbol-X telescope assembly is shown in the case of the “double-disc” shielding option. The difference with the respect to the “simple tube” configuration shown in Figure 2 is the presence of the two co-planar and concentric discs of radius R_1 and R_2, placed at height H_1 and H_2 respectively, above the detection plane.

4. Design trade-off studies: whole detector case

In order to investigate the spectrum of possible design trade-off scenarios, we have started the analysis by exploring the variation of Ω_{CXB} for different H-R_{skirt} values using the trigonometric approach indicated in Section 3. Figure 2 indicates that the residual Ω_{CXB} varies for different positions on the detection plane, and, for a given shield geometry, it is lower toward the centre of the detector. For this reason we have assumed a conservative approach, considering a position on the detector corresponding to the edge of the field of view.
The results are plotted in Figure 4, which shows how Ω_{CXB}, calculated at the edge of the field of view (i.e. at its maximum value), depends upon R_{skirt} (left panel) or H (right panel), for different fixed values of H (left panel) or R_{skirt} (right panel), respectively. The superimposed horizontal lines refer to the maximum allowed Ω_{CXB} required to maintain the aperture background component below 5×10^{-5} (dotted line) and 1×10^{-4} counts cm^{-2} s^{-1} keV^{-1} (continuous line) at 2, 10, and 30 keV.

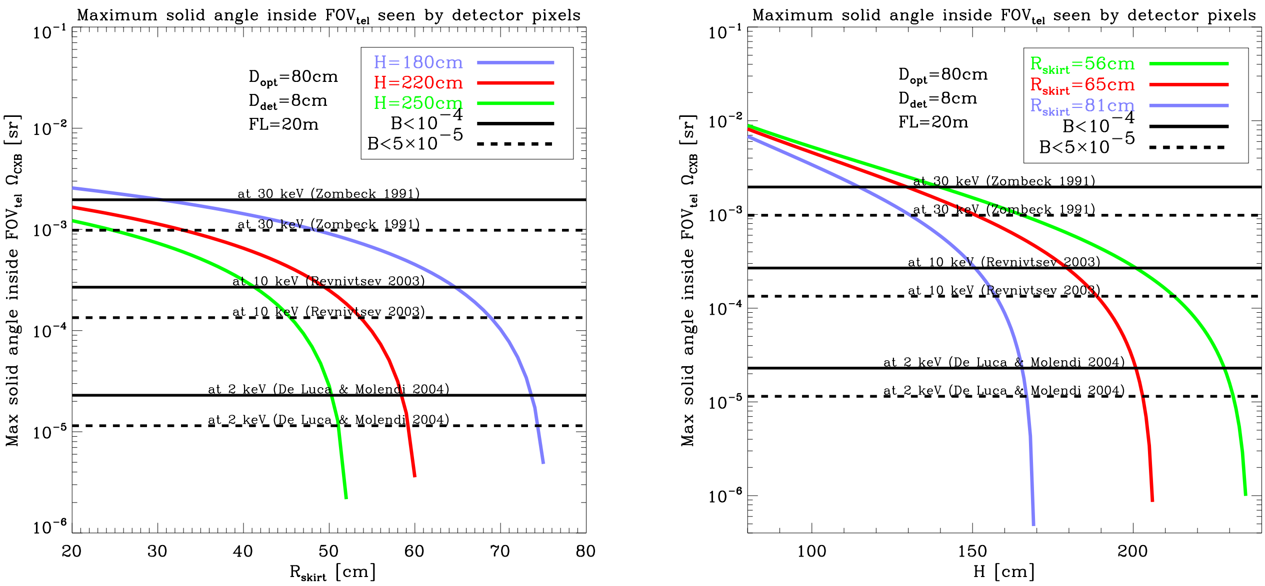

Figure 4:

Ω_{CXB} trade-off studies calculated for a detector position corresponding to the edge of the field of view. (Left panel): Variation of the Ω_{CXB} against R_{skirt} for different values of *H*. (Right panel): Variation of Ω_{CXB} against *H* for different values of R_{skirt}. (Both panels): Horizontal lines indicates the maximum Ω_{CXB} value allowed to maintain the aperture background component below 5×10^{-5} (dotted line) and 1×10^{-4} counts cm^{-2} s^{-1} keV^{-1} (continuous line) at 2, 10, and 30 keV.

Figure 4 allows a detailed design trade-off studies of all the key quantities. For instance (see left panel), assuming a collimator height of *H*=2.2m, a minimum value R_{skirt}~60cm (D_{MSC}~200cm) is needed in order to maintain the aperture background component below 5×10^{-5} counts cm^{-2} s^{-1} keV^{-1} over the entire energy range. On the other hand (see right panel), assuming R_{skirt}=65cm (D_{MSC}~210cm) implies a collimator height of H~205cm to maintain the aperture background component below 5×10^{-5} counts cm^{-2} s^{-1} keV^{-1} always over the entire energy range.

4.1 "Perfect" shielding scenario

As a first assessment of the required shielding dimensions, we have calculated the D_{MSC}-*H* (where *H* can be equivalently replaced by H_2) phase space for reaching a complete ("perfect") shielding of the detection plane, i.e. $\Delta\theta=0$. This is shown in Figure 5, where also the mass of the absorber (i.e. without the needed support structure) is shown. Two points have been highlighted in Figure 4: in the case for instance of *H* (or H_2) = 2.5m, the corresponding MSC shielding quantity is D_{MSC}~1.9m or R_{skirt}~55cm.
For this configuration (and also for $H=H_2$=2m), we have calculated the associated absorber mass, assuming a Tantalum main absorber, with a Tin-Copper-Aluminium-Carbon grading sequence in order to have the last fluorescence line energy outside the Simbol-X energy range. The thickness of the main absorber has been calculated considering (conservatively) only normal incidence angles, and requiring 99% efficiency at 40 keV. The thickness of each grading layer has instead been calculated requiring 99% efficiency at the Kα energy of the preceding material (again a conservative assumption, given the isotropic emission of the fluorescence line). The result shows that the required skirt mass is ~30kg, while the mass of the DSC baffling ranges from ~5 to 18 kg, going from a double-disc to a simple tube geometrical configuration.
It is to be underlined that, in particular for the DSC baffling system, the support structure mass is expected to be greater (factor 1-2) than the main absorber.

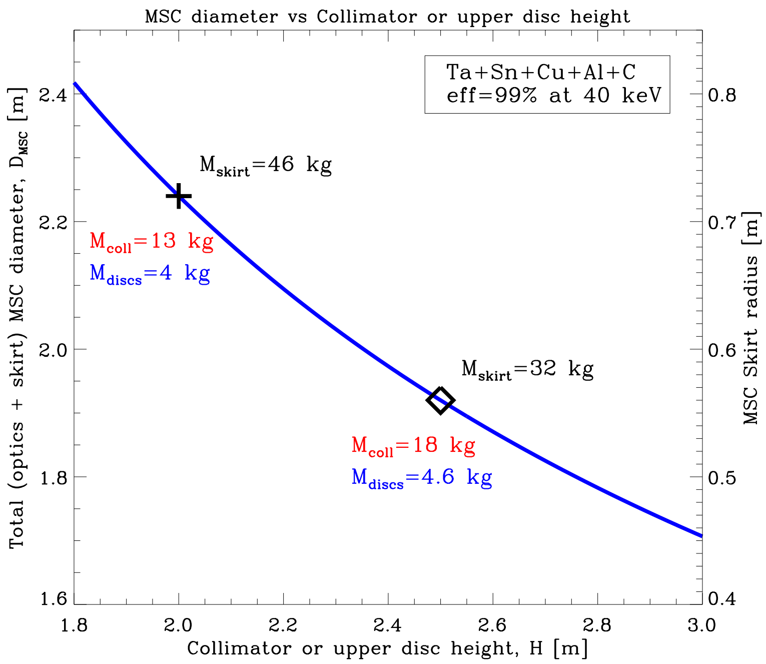

Figure 5:

Total (optics + skirt) MSC diameter, D_{MSC} (left hand Y axis), and MSC skirt radius, against collimator, H, or upper disc height, H_2, (right hand Y axis). The absorber (i.e. without the necessary support structure) mass has been calculated for two values of H: 200, and 250 cm. For each value the DSC baffling system mass has been calculated for the “simple tube” (**red**) and for the “double-disc” (**blue**) geometry. The thickness of the shields has been calculated for Tantalum ad the main absorber, and in order to have a 99% absorbing efficiency at 40 keV, assuming (conservatively) a normal incidence angle. The grading material thicknesses have been calculated to reach 99% absorption at the K_α line energy of the preceding material.

As a partial cross-check, it is worth noting that, for the case of “perfect shielding”, i.e. $\Delta\theta=0$, our results are not in agreement with the indications presented in the *“Detector Satellite / Mirror Satellite Interface Requirements Document”* (00-TS-00013-013-CNES) currently being re-edited at JPO level. In this document, in fact, the suggested technical requirements are of a “sky baffle diameter”>3m[*], coupled with a “collimator length”>1.5m. Figure 3 shows in fact that this specified combination of values would translate in an over-shielding of the background aperture component.
In order to understand this apparent contradiction, we have then repeated the exercise done for Figure 5, but for the “perfect shielding” case, i.e. for $\Delta\theta=0$. The results are shown in Figure 6, which indicates that the collimator-skirt values suggested in the current version of the *“Detector Satellite / Mirror Satellite Interface Requirements Document”* (00-TS-00013-013-CNES) document refer to one of the previous tentative baselines for the Simbol-X mission (i.e.: *FL*: 30m, D_{opt}: 60cm, D_{det}: 6cm).

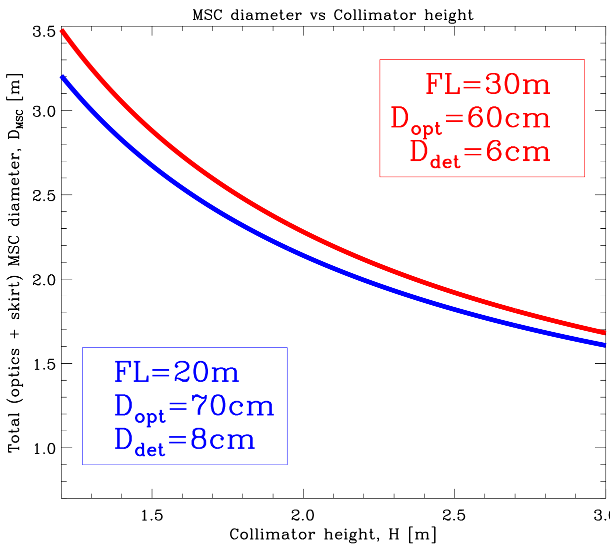

Figure 6:

D_{MSC} vs H in the case of “perfect baffling” ($\Delta\theta=0$) for the current vs previous Simbol-X baseline design.

[*] The quoted document does not give a precise definition for the “sky baffle”, but it is probably to be assumed to be equivalent to the quantity D_{MSC} defined in the present report. Therefore, D_{MSC}>3m corresponds to R_{skirt}>115cm.

It should be noted that the Y axis of Figure 6 shows the *total* MSC diameter, i.e. $D_{MSC}=D_{opt}+2R_{skirt}$, so that, since we are comparing two scenarios with different D_{opt}, the resulting ΔR_{skirt} is greater that the ΔD_{MSC} shown in the figure.

5. Design trade-off studies: detection plane non-uniformity analysis

The analytical approach introduced in Section 3 and developed in Section 4 is in fact somewhat simplistic, since it considers as representative of the whole detection plane the points corresponding to the maximum of Ω_{CXB}. On the other hand the results shown in Figure 5 are probably too conservative since assume a "perfect" (i.e. total) shielding over all the detection plane.

We have thus repeated the evaluation, studying, for both the "simple tube" and "double disc" geometries, the variation of Ω_{CXB} across the detection plane (and therefore across the Simbol-X telescope field of view projected at a distance *FL* on the detection plane) for a sample of DSC and MSC baffling dimensions. This is then translated into the corresponding expected background count rates for different energies. For this approach, a square geometry of the detector has been assumed, together with a circular/cylindrical shape for the collimator and the MSC skirt. The envisaged ±1cm dithering of the DSC with respect to MSC has been, at least in this first evaluation, not considered.

The results are shown in Figure 7, which reports for two geometrical configurations (Top panels: *H*, or H_1 in the case of the double-disc geometry, =200cm and R_{skirt}=65cm; Bottom panels: $H=H_2$=250 and R_{skirt}=50cm), and two energy values (E=3keV; E=30keV), the expected CXB count rate variation over one quarter of the detection plane. For each panel, the super-imposed yellow line corresponds to the edge of the 12 arcmin FOV at *FL*=20m[†]. Moreover, for both the selected geometrical combinations, the skirt mass budget is given.

Figure 7 shows how by increasing the height of the collimator (or, equivalently, of the top circular disc) by 50cm, it is possible to decrease by ~30% the skirt absorber mass, always retaining approximately the same expected CXB counting rate.

As a synoptic view of these results, Figure 8 shows the fraction of detector area (and of the corresponding telescope field of view) against the expected CXB component rate. This has been calculated for two geometrical configurations (*H*, or H_2, =200 and 250cm; R_{skirt}=65, 50 cm), and two energy values (3 and 30 keV). In each of the two panels, the red (blue) vertical line indicate the expected count rate at 30 keV (3 keV), at the detector position corresponding with the edge of the field of view.
We then have that for *H* (or H_2) =250cm and R_{skirt}=50cm, also at 3 keV more than 70% of the detection plane is below 10^{-4} counts cm^{-2} s^{-1} keV^{-1}, while if we consider only the detector area in the telescope nominal field of view, the expected count rate is always below 7×10^{-5} counts cm^{-2} s^{-1} keV^{-1}.

[††] It is worth noting that, assuming the foreseen ±1cm dithering, a fraction, even if small, of the telescope field of view might fall outside the detection plane.

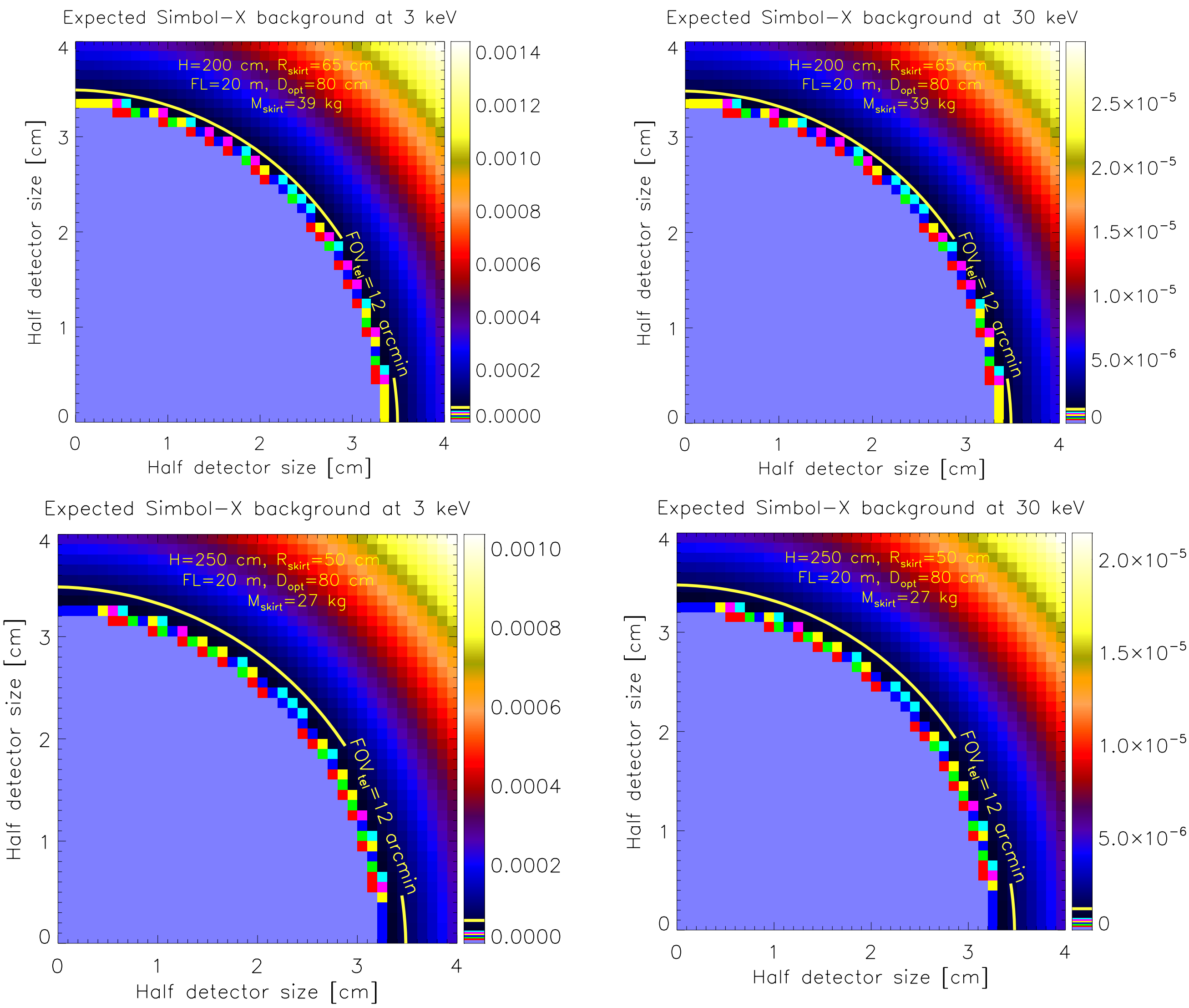

<u>Figure 7:</u>

Expected cosmic X-ray background aperture component variation across the detection plane (1 mm^2 sampling) expressed in *counts* cm^{-2} s^{-1} keV^{-1} (see right hand scale of each colour map) for two possible geometries and two energy values. For all cases it has been adopted: Focal Length= 20m, D_{opt}=80cm.

Energy:

(Left panels): E = 3 keV.

(Right panels): E = 30 keV.

Geometry:

(Top panels): H = 200 cm, R_{skirt} = 65 cm.

(Bottom panels): H = 250 cm, R_{skirt} = 50 cm.

To optimize clarity, the panels show only one representative quarter of the detection plane. X and Y axis are in cm, and in each panel the superimposed yellow continuous line corresponds to the edge of the 12' Simbol-X field of view (FWHM) projected for a 20m focal length.

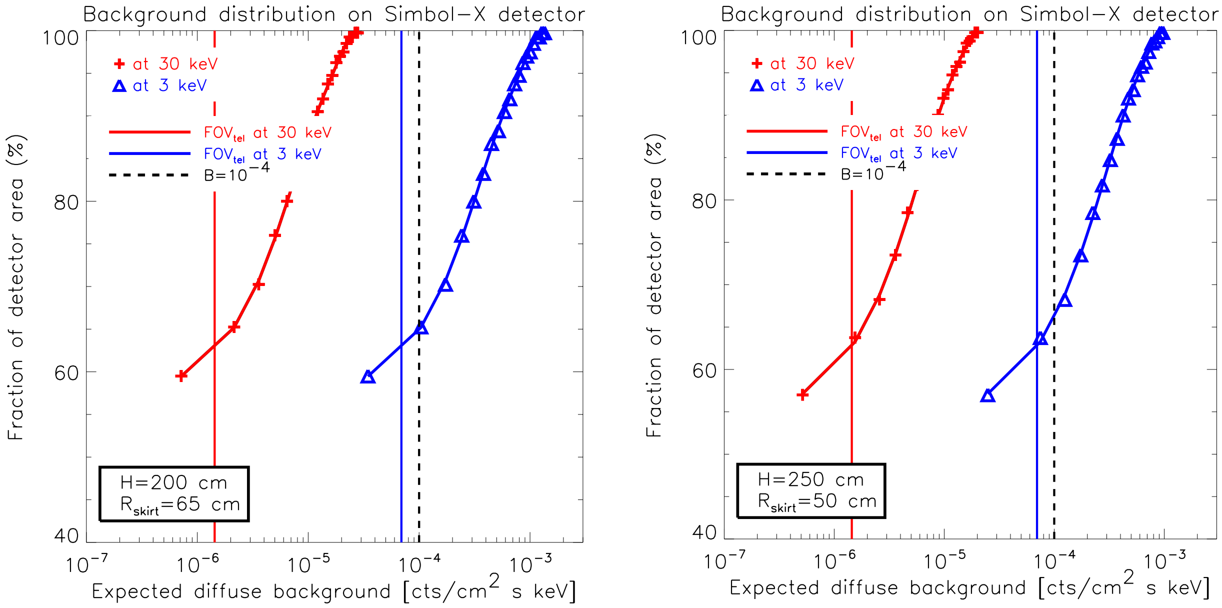

Figure 8:

Fraction of detector area (and associated telescope field of view) against the expected CXB background component count rate at 3 (blue triangles) and 30 (red crosses) keV. The **blue** (**red**) vertical line indicate the expected background rate at the edge of the field view at **3** (**30**) keV. The vertical dashed line indicate the required limit of 10^{-4} counts cm^{-2} s^{-1} keV^{-1}.
(Left panel): H (or H_2) = 2m; R_{skirt}=65cm.
(Right panel): H (or H_2) = 2.5m; R_{skirt}=50cm.

5. Conclusions

The impact of the Simbol-X core scientific objectives on the shielding requirements have been briefly addressed.
The implications on the maximum allowed aperture background component have been translated into maximum detector opening angle, and then into possible DSC vs MSC baffles design trade-offs.
First results indicate that a combination of a DSC baffle (collimator) of height H~2m, with a MSC skirt of radius R_{skirt}~0.7m, would ensure an aperture background component <5×10^{-5} counts cm^{-2} s^{-1} keV^{-1} down to 3 keV.

For the conservative approach of a complete shielding, the mass of the absorber is, in first approximation (see below the foreseen future fine tuning evaluation activity), for H (or H_2)=2.5m and R_{skirt}=55cm, of the order of 32kg for the MSC, and 18 or 4.6 kg for the DSC, in the case of a simple tube or double disk geometry, respectively.
These mass budgets *do not* include the associated needed support structure, the design of which is currently under engineering study for the various proposed configurations.

Further detailed trade-off studies are then needed in order to:

- Optimize the sharing of the CXB shielding between DSC and MSC.
- Evaluate the design and mass envelope of the support structures for both DSC and MSC, for the various possible geometries.
- Include the effect of DSC dithering.

The key activities will have to consider:

- Maximum tube (or top disc) height, feasible for the DSC baffling system.
- Mass of the DSC baffling absorber for the double disc option with respect to the “classical” simple tube.
- Mass of the associated DSC baffling support structure for the two cases.
- Refining of the absorber mass evaluation, considering the possibility of a decreasing thickness for DSC baffling, and the absorption caused by the support structure.
- Sharing of the shielding factor (solid angle and efficiency), and associated mass budget, between DSC and MSC.

6. References

I. De Luca G., & Molendi S., 2004, *“The 2-8 keV cosmic X-ray background spectrum as observed with XMM-Newton”*, A&A, 419, 837

II. Gruber, D., et al. 1999, “*The Spectrum of Diffuse Cosmic Hard X-Rays Measured with HEAO 1”*, ApJ, 520, 124

III. Lumb, D., et al. 2002, *“X-ray background measurements with XMM-Newton EPIC”*, A&A, 389, 93

IV. Malaguti, G., et al. 2005, *“Active and passive shielding design optimization and technical solutions for deep sensitivity hard x-ray focusing telescopes”,* Optics for EUV, X-Ray, and Gamma-Ray Astronomy II. Edited by Citterio, O.; O'Dell, S. L. Proceedings of the SPIE, Volume 5900, pp. 159-171

V. Revnivtsev, M., et al. 2003, *“The spectrum of the cosmic X-ray background observed by RTXE/PCA”*, A&A, 411, 329

VI. Zombeck, M.V., “*Handbook of space astronomy and astrophysics”*, Cambridge: University Press, 1990, 2nd ed.